JOURNAL OF MATERIALS SCIENCE 31 (1996) 6325–6332

A simple method for the preparation of plasma-sprayable powders based on ZrO_2

PARVATI RAMASWAMY, S. SEETHARAMU
Materials Technology Division, Central Power Research Institute, Bangalore 560 094, India
K. B. R. VARMA, K. J. RAO*
Materials Research Centre, Indian Institute of Science, Bangalore 560 012, India

Plasma-sprayable powders of calcia, magnesia and yttria-stabilized zirconia have been prepared by using polyvinyl alcohol binders. The powders have been characterized for sprayability by spray coating on steel plates previously coated with an NiAl bond coat. The suitability of these coatings for thermal barrier applications have been examined. Thermal barrier and related properties, along with phase stability and mechanical properties, have been found to be good. Failure of the thermal barrier coating has been observed to occur at the interface between the bond coat and the substrate, due to the formation of a pile-up layer consisting of Fe–Zr–Al–O compound.

1. Introduction

Plasma spraying of powders depends on several factors. Important among them are the grain size and its distribution, morphology and flowability, chemical composition and substrate surface condition. It is essential that the chemistry of the sprayable powder is unaffected by the high-temperature plasma in which it melts. It should not undergo undesirable changes, such as degradation, component sublimation or oxidation/reduction reactions [1]. Various manufacturing processes are being adopted to prepare commercial grade powders. They involve spray drying, high-temperature sintering and even fuse and crush methods [2]. A new attrition mill process, which binds component powders mechanically into spray powder particles, has been recently reported [2]. On comparison of a few powder manufacturing processes, it is understood that the process using binders and spray drying gives high (60%–80%) yield and is economically attractive [2]. Chemical routes for the preparation of powders such as emulsion precipitation [3] and gel decomposition have also been examined and the resulting coatings have been characterized [4]. These processes are at present not cost effective.

In classical ceramic processing, the role of organic binders used in powder preparation (granulation) is well documented [5]. However, very little is known about the application of this conventional method to prepare plasma-sprayable powders. In this paper, we report a method of preparation of such plasma-sprayable grade powders which is simple, cost effective and gives rise to substantially high yields. The suitability of the powders for plasma-spray application has been investigated for the case of zirconia (ZrO_2)-based thermal barrier coatings (TBC) [6–8].

TBCs, in general, consist of an outer thermally insulating ceramic oxide layer and an inner oxidation-resistant metallic bond coat [9]. ZrO_2-based ceramics have been in the forefront for TBC applications [8, 10, 11]. Pure ZrO_2 is unsuitable due to the incidence of large volume change and associated cracking during its tetragonal to monoclinic transition around 1370 K [12] during cooling. This problem is generally eliminated by stabilizing either partially or fully, the high-temperature cubic/tetragonal (c/t) phase by doping monoclinic ZrO_2 (m-ZrO_2) with CaO, MgO or Y_2O_3 [13–15]. The most prominent commercially available compositions are 8 wt % Y_2O_3–ZrO_2 (AMDRY-6610), 18–26 wt % MgO–ZrO_2 (AMDRY 333) and 5 wt % CaO–ZrO_2 (AMDRY 6700). These compositions have been studied extensively [16–18]. The ZrO_2-based coatings fail at high temperatures and the failure is attributed to (i) the reversion of c/t phase to m-ZrO_2 [8, 17–19], (ii) oxidation of the intermediate bond coat/substrate, and (iii) the thermal expansion mismatch between metal and ceramic layers [8].

In the present work, the c/t phase of ZrO_2 compositions have been stabilized by introduction of an additional step to the conventional method of preparation and that is by heating to high temperatures in an oxy-acetylene flame which provides a slightly reducing atmosphere. The powders have been made sprayable by using polyvinyl alcohol (PVA) as a binder and characterized for their flowability and particle-size distribution from the point of view of the plasma sprayability. The sprayed coatings have been evaluated for thermal barrier effect, adhesion strength and hardness. The nature of the phases present, the coating stabilities and microstructures have also been examined.

* Author to whom all correspondence should be addressed.

0022–2461

TABLE I Powder compositions

	Designation	Compositions (wt %)				Others	
		ZrO_2	MgO	CaO	Y_2O_3	Al_2O_3	SiO_2
1	Y	92.0	–	–	8.0	–	–
2	M	72.0	25.0	1.5	–	–	1.5
3	C	94.0	–	5.0	–	0.5	0.5

TABLE II Typical spray conditions (for Y compositions)

Spray parameters	Settings
Argon	44 l min^{-1}
Hydrogen	13 l min^{-1}
Powder gas (Ar)	3.4 l min^{-1}
Current	630 A
Voltage	70 V
Injector diameter	1.8 mm
Injector angle	90°
Injector distance	6 mm
Powder feed rate	40 g min^{-1}
Nozzle diameter	6 mm
Spray distance	120 mm
Air cooling (substrate)	Yes

2. Experimental procedure

2.1. Powder preparation

Powders of m-ZrO_2 (99.0%) and Y_2O_3 (99.9%) were procured from Indian Rare Earths Ltd. MgO, $CaCO_3$, Al_2O_3 and SiO_2 (all 99% or higher purity) were obtained from LOBA Chemie. Table I shows the initial powder compositions.

The preparation of plasma-sprayable grade powders consisted of the following steps.

(i) Raw materials were weighed to an accuracy of 0.01 g and wet ball milled in agate media for 24 h and the slurry was oven dried at about 423 K. These powders were calcined at 1423 K for 12 h and the product was again ball milled for 4 h; the slurry was oven dried. The dominant particle size at this stage was found to be about 1–2 μm.

(ii) The dried powder was mixed with 10% polyvinyl alcohol (PVA) and compacted into flat rectangular bars (100 mm × 100 mm × 5 mm).

(iii) The bars were heated to about 2073 K in an oxy-acetylene flame. Then it was ball milled for about 8 h and the slurry was oven dried.

(iv) Small agglomerates of the powder were formed by mixing the powder composition with 10% PVA in a planetary mixer, and then oven dried for 2–3 h in order to remove the moisture.

(v) To retain particles with sizes ranging from 45–90 μm, the dried powder was sieved through 170 and 300 mesh. The powder compositions thus prepared were used for plasma spraying.

2.2. Characterization of powders

The present process has resulted in a yield of about 80% plasma sprayable powder.

The powders were analysed for flowability by measuring the flow rate using the standard JIS Z 250 2. The measurement was done by allowing a known weight of the sample powder to flow through a flow meter and measuring the time taken for the entire powder to flow through the funnel orifice. The formation of the c/t phases of ZrO_2 was confirmed by X-ray diffractometry (XRD) using Philips PW 1710 with CuK_α radiation. The particle size analysis was carried out on a particle size analyser (Malvern Mastersizer X version 1.2). The morphological features were studied by scanning electron microscopy (SEM) using a Cambridge Stereoscan 360.

2.3. Spray-coated specimen preparation

Flat plates (75 mm × 25 mm × 2.5 mm) and buttons (25 mm diameter × 10 mm) of mild steel were used as substrates. One side of the substrate was initially cleaned, degreased and subjected to grit blasting. This was followed by spray coating of 75–100 μm thick bond coat of commercial nickel-5 aluminide (AMDRY-956) powder using Plasma Technik (80 kW) spray system. The oven-dried powders of thermal barrier material were spray coated upon the bond-coated substrates. Table II shows the typical spray conditions for Y composition.

2.4. Characterization of coatings

The nature of the ZrO_2 phases present in the coatings was also examined using XRD. Mechanical properties such as adhesive strength and Vickers' hardness of the cross-section were determined by using standards ASTM C 633–69 and DIN 51 303, respectively. Measurement of adhesive strength was carried out for a button substrate coated on one side, bonded to two pull rods with a strong resin and pulled under tensile load. The weaker ceramic–substrate interface fails, and the corresponding load/area is taken as a measure of adhesive strength. Microstructure was examined using SEM.

The most widely employed (standard) test for evaluation of TBCs makes use of a simulated environment involving a burner test rig [6, 9]. However, accelerated thermal cycling tests using furnaces [4] and oxy-acetylene torches [7] are also frequently adopted. In the present work, for studying thermal shock resistance and thermal barrier, a special test facility using an oxy-acetylene torch has been established for the purpose. In this set-up, the test specimen is thermally insulated on all its edges using low-mass alumina ceramic fibre and an area of about 15 mm × 10 mm is left uncovered on both metal (uncoated) and ceramic (coated) sides. A torch of oxy-acetylene flame (temperature of 1273 ± 10 K) is focused on to the ceramic coating and held for about 30 min. After the steady state is established, the temperature drop across the coating is determined by measuring the temperature of the metal on the other side using a K-type (chromel–alumel) thermocouple and an optical pyrometer. Following this, the flame is put out and compressed air is blown to lower the surface temperature

TABLE III Flow rates and coating thicknesses

Powder designation	Flow rate ($g\,min^{-1}$)	Coating thickness (μm) (inclusive of 75–100 (μm) NiAl)
Y	40	325–350
M	50	475–500
C	75	575–600

rapidly. This process of imparting thermal shock is repeated until visible cracks appear on the surface. The number of such thermal cycles which the TBC is able to withstand before failure, and the temperature drop across the barrier during the tests, are recorded.

3. Results and discussion

3.1. Flow rate and coating thickness

Table III shows the flow rates of the powders during spraying and the coating thicknesses of the compositions. It may be noted that spray coating was performed with identical number of passes across the substrates for all the compositions investigated. The coatings were found to be smooth and they were used in the as-sprayed condition for other tests.

Y, M, and C possess coating thicknesses in increasing order, consistent with the flow rates of these compositions which, in turn, may be due to variations in the densities of samples under study. The use of PVA as binding agent between the particles hinders the process of compaction and densification.

3.2. Phase analysis

Fig. 1 shows the XRD patterns of (a) calcined powder, (b) sprayable powder and (c) plasma-sprayed coating of a typical composition Y. The phase fractions of m and c/t were determined by the Polymorph technique [20] in which $X_{c/t}$, the phase fraction of the c/t phase, is given by

$$X_{c/t} = I_{c/t(1\,1\,1)}[1/(I_{m(1\,1\,1)} + I_{m(1\,1\,\bar{1})} + I_{c/t(1\,1\,1)})] \quad (1)$$

where I_m and $I_{c/t}$ are the intensities of the reflections corresponding to the monoclinic and cubic/tetragonal phases, respectively. The percentages of c/t phase present in the calcined powders, spray powders and the coated samples, are presented in Table IV. The results indicate that only partial stabilization of the c/t has occurred in calcined and sprayable powders, the extent of stabilization being higher in the case of sprayable powders. However, in the TBC layers, complete or near complete stabilization of c/t phase of ZrO_2 has been observed. The passage of the powder through the plasma and the interfacial interaction with the substrate appear to enhance the degree of stabilization of c/t phase in the coated films. The percentage of c/t phase in the coatings obtained from M and Y compositions is found to be identical to those obtained from commercial grade powders of the same compositions.

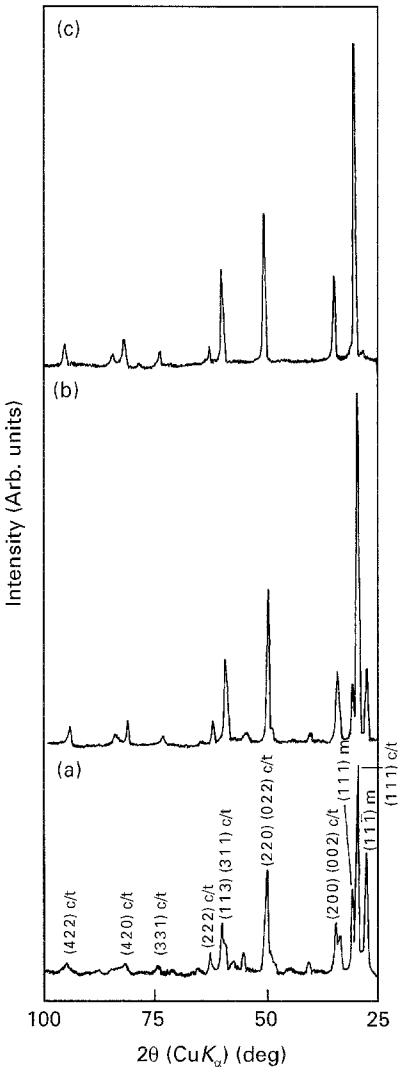

Figure 1 X-ray diffractograms of Y: (a) calcined powder, (b) sprayable-powder, and (c) plasma-sprayed coating.

TABLE IV Percentage phase fractions

	Designation	Cubic/tetragonal phase fraction (%)		
		Calcined powder	Spray powder	Coating
1	Y	52	75	> 95
2	M	57	75	100
3	C	60	95	100

It is well known that the stability of the plasma-sprayed coatings derives from the tetragonal phase of zirconia alloys, containing 4–12 wt % yttria, and which does not transform to the monoclinic phase upon cooling to room temperature [8, 21, 22]. This phase, however, decomposes at elevated temperature (> 1673 K). A typical 8% Y_2O_3–ZrO_2 coating may be used without degradation up to 1623 K. The 24% MgO–ZrO_2 composition is known to decompose even around 1223 K with rapid precipitation of MgO [8].

In XRD patterns, the peaks due to cubic and tetragonal ZrO_2 overlap and we have not deconvulated the peaks in the present work. In any event, it is the

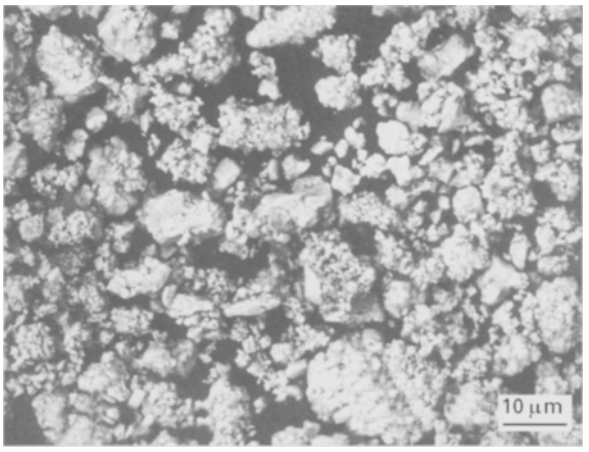

Figure 2 Scanning electron micrograph of plasma-sprayable powders of Y.

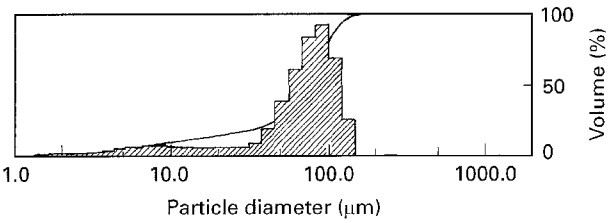

Figure 3 Particle-size analysis of Y.

destabilization of the c/t phases at higher temperatures which causes the undesirable reduction of the coating life, and hence the stability of the coatings on exposure to high temperature (1273 K) for long duration (500 h) has been investigated and is discussed in subsequent sections.

3.3. Microscopy and particle-size analysis

The average particle size of the starting ball-milled powder (before addition of the binder) was about 1–2 μm and the maximum size was below 8 μm. Such fine powders are not suitable for plasma spraying because the particles tend to stick together. The plasma-sprayable powders prepared here are actually agglomerates of these fine powders with particle size 40 μm and above. Fig. 2 shows a scanning electron micrograph of a typical sprayable powder of Y. Particle-size analysis, carried out on the spray powders in the completely dry state, indicated that the average particle size is about 73 μm, which is known to be highly suitable for plasma-spraying purposes. Typical particle-size distribution data are shown in Fig. 3.

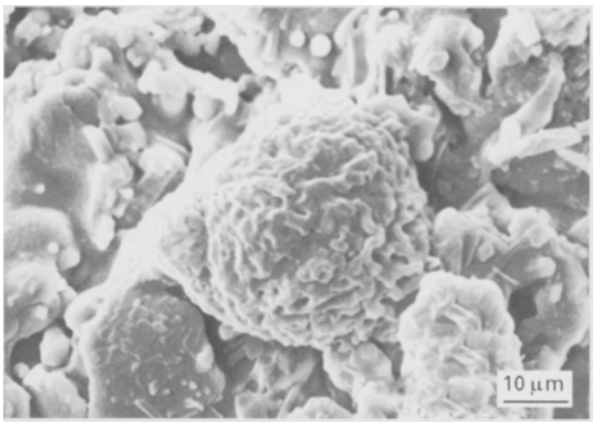

Figure 4 Scanning electron micrograph of as-sprayed surface of Y.

The scanning electron micrograph of the as-sprayed surface of Y is shown in Fig. 4. The presence of grains measuring 3–5 μm, the formation of random clusters and a smooth surface (indicative of possible melting), are some of the salient features of the coated surface.

Although the spray powder is coarse, the coating possesses a fine-grained microstructure. This is because of the release of the fine particles from the agglomerates during evaporation of the polymeric binder (PVA) on interaction with the plasma.

3.4. Mechanical properties

The adhesive strength of the coatings and Vickers hardness values are listed in Table V. The probable mode of failure is also indicated in the same table. Results pertaining to coatings from commercial 8% Y_2O_3–ZrO_2 (Plasma Technik, PT-1085) are also included for comparison purposes. It may be noted that the adhesive strength of resin used for bonding the specimen to the pull rod was about 70 MPa. While all the Vickers hardness values measured on the coatings Y and C (ten measurements on each specimen) exhibited little variation from the average values, a large distribution of hardness values has been noticed in specimen coated with M. This may be due to the higher porosity of these coatings as compared to Y and C. The Vickers hardness values of the coatings from commercial powders of equivalent compositions obtained under identical test conditions are higher by about 10%. This may again be due to higher porosity present in samples Y, M and C resulting from burning out of residual polymer or its carbonized products. The bond strengths of all three compositions Y, M and C are seen (Table V) to be excellent. The

TABLE V Mechanical properties of the coated specimens

	Designation	Adhesive strength (MPa)	Vickers hardness number (VHN), 0.2 kg load	Remarks on the probable mode of failure
1	Y	> 70	590	Resin strength
2	M	45–55	475 ±25	Ceramic strength
3	C	35–40	585	Ceramic strength
4	PT-1085	60	600	Ceramic strength

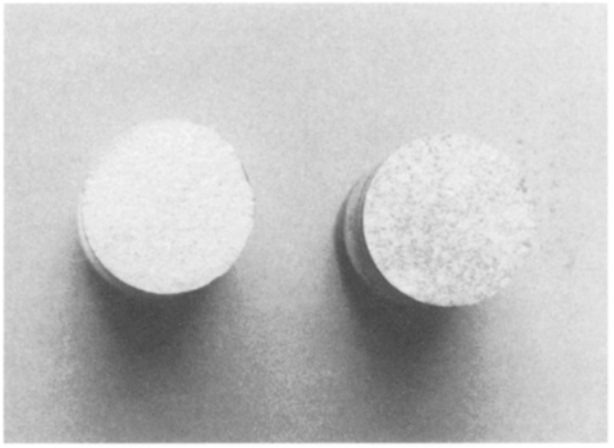

Figure 5 Photograph of pull rod after the adhesive strength test (of M).

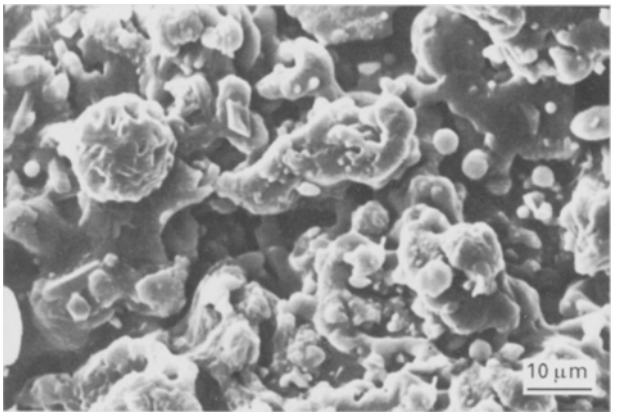

Figure 6 Scanning electron micrograph of Y, failed after thermal cycling.

TABLE VI Thermal shock and thermal barrier properties of coatings

	Designation	Number of thermal shock cycles to failure	Temperature drop across barrier at hot zone[a], temperature = 1273 ± 10 K	
1	Y	35	623 K (573 K	573 K 548 K)
2	M	35	573 K (523 K	523 K 473 K)
3	C	38	523 K (498 K	523 K 498 K)
4	PT-1085	35	573 K (533 K	573 K 523 K)

[a] Temperatures were measured using a chromel–alumel thermocouple. Temperatures given in parentheses refer to measurements using an optical pyrometer.

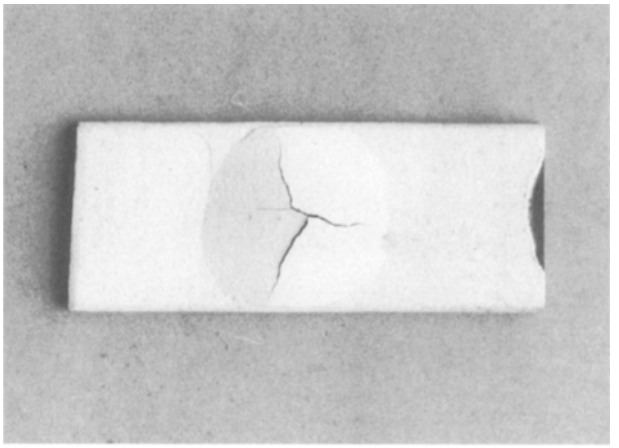

Figure 7 Photograph of thermal shock cycled specimen after failure.

surface of the pull rods after performing the strength test on M and C showed that the failure occurs within the ceramic itself. A photograph of a typical surface after the test is shown in Fig. 5. In the samples of Y, however, the surfaces of the pull rods consisted of only the resin on one side and the coating was found to be intact on the button itself, suggesting that the failure occurs in the resin and not in the ceramic coating. The accurate strength of the coating and mode of failure could not be determined owing to non-availability of a resin having a strength higher than 70 MPa. The coatings prepared from powders Y, M and C exhibit equivalent or improved properties compared to those made from commercial grade powders.

3.5. Thermal properties

Evaluation of the plasma-sprayable powders prepared by the binder method through the study of the thermal barrier and thermal shock resistance of their coatings is the principal focus of this work. The data related to the thermal barrier and thermal shock properties are summarized in Table VI. The number of thermal shock cycles that the various coatings are able to sustain when cycled between 1273 K and room temperature in the manner described earlier, are given in the table. For comparison, the data generated for a coating from commercial 8% Y_2O_3–ZrO_2 powder (Plasma Technik, PT-1085) tested under similar conditions is also given. There are two barrier drop temperatures given in the table. They refer to the averages of the first and last five values, respectively, of the data collected during each thermal cycle before failure occurred. An examination of the thermal data obtained from coatings of different thicknesses revealed the following points.

(a) Although the coating thicknesses vary widely (325 μm in the case of Y, 600 μm in the case of C and 500 μm in the case of M), the number of thermal shock cycles does not vary significantly.

(b) In spite of possessing the lowest thickness among the coatings investigated here, composition Y seems to exhibit the maximum temperature drop across the ceramic. This reconfirms the role of Y_2O_3 in enhancing the thermal barrier effect of stabilized ZrO_2. Fig. 6 shows a scanning electron micrograph of a typical failed specimen of Y. The occurrence of considerable grain disintegration compared to the as-sprayed specimen (Fig. 4) during thermal shock cycling, and the formation of wide gaps is seen in the failed specimen. Fig. 7 shows a photograph of a thermal shock cycled specimen soon after failure. The mode of

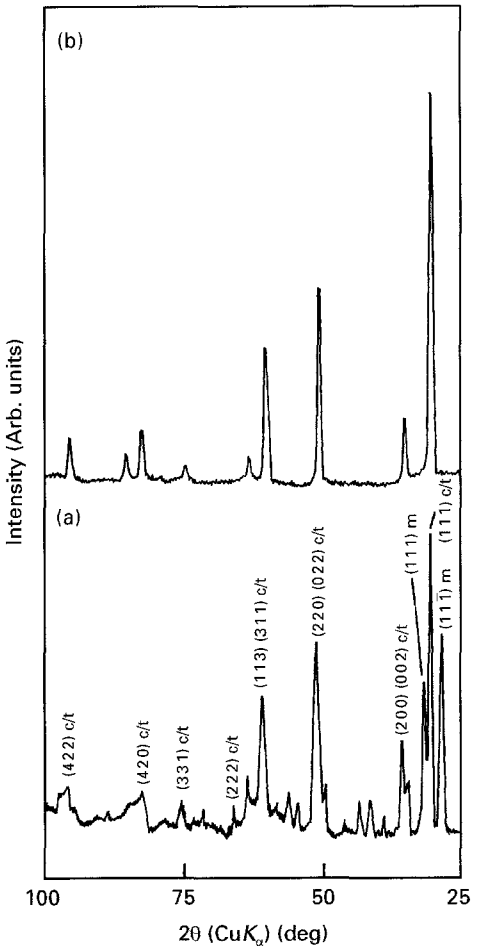

Figure 8 X-ray diffractograms of coatings after heat treatment at 1273 K for 500 h (a) M and (b) Y.

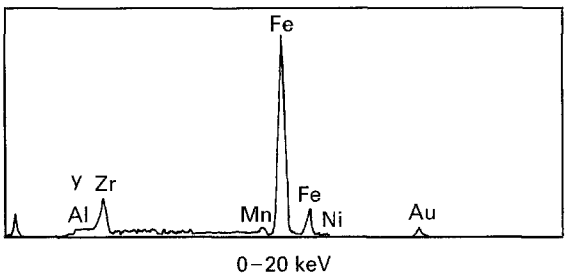

Figure 9 EDAX analysis of the metal–ceramic interface of failed specimen Y.

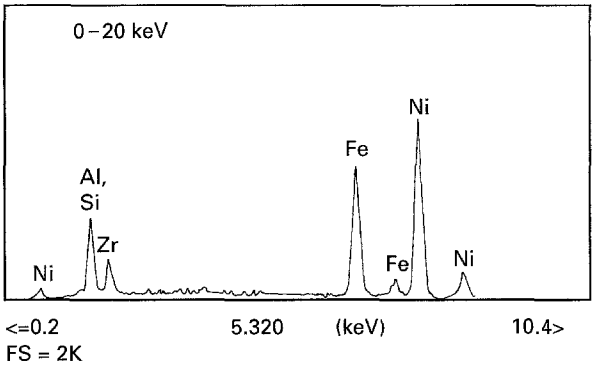

Figure 10 EDAX analysis of the metal–ceramic interface of failed specimen Y, polished and etched.

failure in all compositions appears to be similar. It seems to occur mainly at the metal (substrate) – ceramic interface, as a consequence of which the coatings are peeled off in the area where the flame has been focused. The appearance of the failed film is suggestive of initial detachment of the top layer from the substrate and subsequent lift off of the film and its cracking under interlayer thermal stresses. This may be mainly due to the degradation (oxidation) occurring in the NiAl bond coat at temperature > 1088 K [23]. The use of a more oxidation-resistant bond-coat material, such as MCrAlY (M = Co, Ni, Fe etc.) may enhance the shock life.

(c) The XRD pattern of the thermal shock cycled ceramic coating of Y is similar to that of the as-sprayed coating of Y. From these studies it is found that the percentage of c/t phase is about 95%. Thus, it is confirmed that absolutely no destabilization of the c/t phase has occurred on failure. A similar trend is observed in the case of coatings of C. However, some destabilization is observed in M.

To further confirm the stability of these coatings, the metallic layers adherent to the coatings of Y, M and C were removed and the ceramic films were heat treated at 1273 K for 500 h in a static air atmosphere. Fig. 8 shows the XRD pattern of (a) M and (b) Y after the exhaustive heat-treatment schedule. Both Y and C (not shown in the figure) showed the absence of m-ZrO_2 indicating complete stabilization of c/t phase. Further, there was absolutely no shift in the d values (lattice spacings) when compared with the d values of the as-sprayed specimens, suggesting that the unit cell remains unaltered. However, in the case of M, considerable change was observed in the percentage of c/t phase, indicating destabilization. Further, some shift in the d values, towards the higher side, tending closer to the d values of c/t phase, was observed. This suggests that on prolonged heat treatment, MgO precipitates out [8] and the rest remains as a part of c/t phase.

(d) The compositional analysis of the metal surface of the peeled-off coating was done using EDAX. Fig. 9 shows the data obtained by such an analysis. The surface consists predominantly of iron with small amounts of zirconium, yttrium, manganese and aluminium while only traces of nickel are seen. The same surface was mildly polished and etched and the EDAX pattern was examined again (Fig. 10). It was seen that the surface was now rich in nickel with zirconium present in somewhat higher proportion. The top surface of the substrate where failure occurred was also similarly examined using EDAX in "as-failed" and after "polish and etch" conditions. The EDAX of the "as-failed" surface was very similar to that shown in Fig. 9, while after "polish and etch", only iron was found to be the dominant element (with traces of manganese).

The above observation indicates that the failure occurred after the formation of a chemically distinct pile-up layer between the bond coat and substrate,

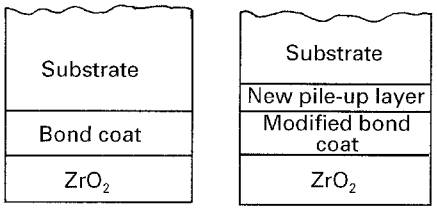

Figure 11 Schematic drawing of the formation of the pile-up layer.

due to diffusion of various elements from the hot zone towards the substrate, as schematically reported in Fig. 11. Firstly, the known mobility of O^{2-} induces it to diffuse into and through the bond coat towards the substrate. Because, in nickel aluminide, nickel carries a slightly negative charge (electronegativity of nickel (1.8) is higher than that of aluminium (1.5)), it holds back O^{2-} ions in the bond coat layer. Therefore, O^{2-} ions do not diffuse effectively further into the substrate. This is followed by diffusion of Zr^{4+} ions. The diffusion is facilitated by the negative charge of advancing O^{2-} ions and a temperature gradient in the right direction. The temperature gradient also helps aluminium atoms in the bond-coat layer to diffuse towards the substrate. At the bond coat–substrate interface, therefore, a pile-up occurs of the above ions which do not migrate further into the mild steel substrate. Thus, after sufficient exposure to the thermal gradient, a new interface develops made up of pile-up ions. This constitutes yet another oxide layer which also acts as a thermal barrier. The result is that the temperature of the bond-coat layer itself is progressively elevated during thermal cycling resulting in a thermal expansivity mismatch which lifts off the TBC film along with the bond coat. The nearly equal number of thermal cycles to failure is also consistent with the formation of the pile-up oxide layer, because a critical build up of the pile-up layer is necessary for the failure, and the critical thickness is determined by the diffusion coefficients of O^{2-}, Zr^{4+} and Al^{3+}, maximum temperature, time of exposure and bond coat thickness. All of these factors remain roughly similar for the various films.

Other degradation mechanisms for ZrO_2–8% Y_2O_3 coatings with M–Cr–Al–Y and aluminide bond coats have been reported in the literature. Apart from destabilization of the c/t phase, the two failure mechanisms involve mechanical failure of the ceramic overcoat and oxidation of the bond coat [8, 19]. The present mechanism is qualitatively different from those in the literature for the following reasons. (a) The oxide layer is not formed as a consequence of the oxidation of the elements in the bond coat layer. (b) It is envisaged that it results from the diffusion of O^{2-}, Zr^{4+} and Y^{3+} ions across the bond coat which pile up between the bond-coat layer and the substrate. This is evidenced from the EDAX studies. The presence of zirconium and yttrium observed in EDAX is a convincing evidence for the proposed mechanism. However, further studies are needed in order to arrive at exact mechanisms. In the present work, it is evident that apart from thermal shock and barrier properties the coatings possess excellent phase and mechanical stability over a long duration of exposure to high temperature. This confirms the suitability of the binder method of preparation of sprayable powders for plasma spraying for TBC applications. However, failure appears to be due to the pile-up layer whose formation can be avoided if choice is made of bond coat material which does not facilitate diffusion of ions constituting the pile-up layer.

4. Conclusions

1. Plasma sprayable powders of 8% Y_2O_3–ZrO_2, 25% MgO–ZrO_2 and 5% CaO–ZrO_2 compositions have been prepared using PVA as binders. This method offers powders with a good (80%) yield.

2. The powders are plasma sprayable and the sprayed coatings are smooth and well adherent to the substrate. They possess high hardness and bond strength. 8% Y_2O_3–ZrO_2 coatings possess superior adhesive strength and equivalent micro hardness compared to similar commercial compositions. These coatings have been evaluated for suitability as TBCs.

3. The coatings exhibit excellent phase stability, thermal barrier and thermal shock-resistant properties. 8% Y_2O_3–ZrO_2 coatings exhibit improved thermal barrier characteristics and thermal shock properties comparable to similar commercial compositions.

Acknowledgement

The authors acknowledge the permission granted by CPRI for publishing this paper.

References

1. W. F. CALOSSO and A. R. NICOLL, 87-ICE-15, in "Energy-sources technology conference and exhibition", Dallas, Texas, 15–20 February 1987 (ASME, New York, 1987) p. 1.
2. S. RANGASWAMY, *Sulzer Tech. Rev.* **2** (1994) 6.
3. FAWZY G. SHERIF and LIEH-JIUN SHYU, *J. Amer. Ceram. Soc.* **74** (1991) 375.
4. M. CHATTERJEE, J. RAY, A. CHATTERJEE, D. GANGULY, S. V. JOSHI and M. P. SRIVASTAVA, *J. Mater. Sci.* **28** (1993) 2803.
5. A. R. TETER, *Ceram. Age* **82**(8) (1996) 30.
6. P. VINCENZINI, *Ind. Ceram.* **10** (3) (1990) 113.
7. N. PERRIN, H. BURLET, M. BOUSSUGE and G. DESPLANCHES, *Surf. Coat. Technol.* **56** (1993) 151.
8. A. BENNETT, *Mater. Sci. Technol.* **2**(3) (1986) 257.
9. R. J. BRATTON and S. K. LAU, in "Advances in Ceramics", Vol. 3 "Science and technology of Zirconia", edited by A. H. Heuer and L. W. Hobbs" (American Ceramic Society, Columbus, OH, 1981) p. 226.
10. S. ALPERINE and L. LELAIT, *J. Eng. Gas Turbines Power Trans ASME* **116**(1) (1994) 258.
11. D. L. PORTER and A. H. HEUER, *J. Amer. Ceram. Soc.* **62** (1979) 298.
12. R. STEVENS, *Trans. J. Bri. Ceram. Soc.* **80** (1981) 81.
13. R. H. J. HANNINK, *J. Mater. Sci.* **18** (1983) 457.
14. J. R. VANVALZAH and H. E. EATON, *Surf. Coat. Technol.* **46** (1991) 289.
15. C. L. CURTIS, D. T. GAWNE and M. PRIESTNALL, *J. Mater. Sci.* **29** (1994) 3102.
16. P. SCARDI, L. LUTTEROTTI and E. GALVANETTO, *Surf. Coat. Technol.* **61** (1993) 52.
17. S. V. JOSHI and M. P. SRIVASTAVA, *ibid.* **56** (1993) 215.

18. R. A. MILLER, J. L. SMIALEK and R. G. GARLICK, in "Advances in ceramics", Vol. 3, "Science and technology of zirconia", edited by A. H. Heuer and L. W. Hobbs (American Ceramic Society, Columbus, OH, 1981) p. 241.
19. B.-C. WU, E. CHANG, S.-F. CHANG and D. TU, *J. Amer. Ceram. Soc.* **72** (1989) 212.
20. R. C. GARVIE and P. S. NICHOLSON, *ibid.* **55** (1972) 303.
21. J. R. BRANDON and R. TAYLOR, *Surf. Coat. Technol.* **39/40** (1989) 143.
22. H. G. SCOTT, *J. Mater. Sci.* **10** (1975) 1527.
23. R. H. UNGER, in "Thermal Spray: Advances in coatings technology", Proceedings of the National thermal spray conference, edited by D. L. Houck, 14 September 1987, Orlando, Florida (ASM International, 1988) p. 365.

Received 6 March 1995
and accepted 2 July 1996